| Journal of Coastal Research | 16 | 3 | 864–869 | West Palm Beach, Florida | Summer 2000 |
|---|---|---|---|---|---|

# Shore-Based Acoustic Doppler Measurement of Near-Surface Currents across a Small Embayment

**George O. Marmorino and Clifford L. Trump**

Naval Research Laboratory
Remote Sensing Division, Code 7250
4555 Overlook Avenue, S.W.
Washington D.C. 20375, U.S.A.

**ABSTRACT**

MARMORINO, G. O. and TRUMP, C. L., 2000. Shore-based acoustic Doppler measurement of near-surface currents across a small embayment. *Journal of Coastal Research,* 16(3), 864–869. West Palm Beach (Florida), ISSN 0749-0208.

Shore-based measurements of near-surface currents are used in a preliminary study of the circulation patterns in a small embayment (width of about 120 m). The measurements were made using an acoustic Doppler current profiler mounted so two acoustic beams scanned horizontally beneath the surface and across the embayment. The data show spatially variable flow patterns that recur at semi-diurnal tidal period but do not vary sinusoidally in time. A similar measurement strategy may prove useful in monitoring the effects on circulation patterns of dredging or jetty construction, studying patterns of pollutant dispersal, or in making an exploratory investigation prior to deploying current-meter moorings.

**ADDITIONAL INDEX WORDS:** *Near-surface current measurement, "horizontal" ADCP measurements.*

## INTRODUCTION

Recently in this journal MORANG, LARSON, and GORMAN (1997) surveyed the techniques commonly used to measure coastal currents. They identify the following three classes of Eulerian methods: HF radar, current meters, and acoustic Doppler current profilers (ADCPs). Respectively, these produce maps of near-surface currents, "point" measurements of the current at a particular depth and horizontal position, and vertical profiles of the current using a sensor deployed either on the bottom or near the surface. Each of these approaches has drawbacks for the study of the circulation in a small embayment or harbor, or across a channel, where the flow field may vary over spatial scales of a hundred meters or less. HF radar measurements, for example, while having the advantages of being made remotely and providing access to the data in nearly real-time, have a relatively coarse spatial resolution of the order of one kilometer (*e.g.,* KOSRO *et al.,* 1997; PRANDLE, 1997). Current meters and ADCPs cannot be safely moored near the surface in highly trafficked areas, and multiple instruments are needed to measure the horizontal variability, adding to cost. Also, data from any type of mooring would have to be telemetered to shore for real-time analysis.

The objective of the present paper is to illustrate how an acoustic Doppler current profiler of the type in general use by the oceanographic community may be used to measure a "horizontal profile" of the near-surface current. One advantage of this approach is the instrumentation may be deployed from the relative safety of the shore. Another is accessibility to the data so results may be obtained during the deployment, thus giving the investigator the option of changing the sampling strategy. Thus we illustrate a somewhat new application of existing technology to the problem of measuring nearshore currents.

## STUDY AREA AND INSTRUMENTATION

The area of study is a small basin or embayment located in the southern part of the Delaware Bay (Figure 1). Outside the mouth of the embayment is a junction of three "channels". To the northeast is Roosevelt Inlet, which provides a connection to the bay. The inlet is protected by rock jetties and has a depth of 4 m at high tide. (The tidal range in the study area is about one meter.) To the northwest is the Broadkill River, which drains a large area of tidal marshes and has flow speeds during ebb estimated to be 50 to 75 cm/s. Connecting from the southeast is a navigable canal, which runs through the town of Lewes. The embayment itself has a width of about 120 m, an approximate surface area of $2 \times 10^4$ m$^2$, and an average depth less than 3 m. The mouth of the embayment is approximately 70 m wide and has a mean depth of about 2.5 m; the cross-sectional area of the mouth is thus about 175 m$^2$. Numerous areas of shoals, weed beds, and bars are present in the area, and regions of hydraulic phenomena (*e.g.,* tidal rips) occur.

The ADCP used in this study is a 307-kHz narrowband unit manufactured by RD Instruments. The ADCP was clamped at 0.6-m depth to a vertical support pole located on the port side of the R/V Cape Henlopen, about 3.5 m off the ship's centerline. (The pole is typically used to mount a downward-looking 1200-kHz ADCP for underway measurements.) The ship was docked at the University of Delaware's College of Marine Studies on the eastern side of the embayment (Figure 1). The ship provided a convenient source of electrical power

*98182 received 13 July 1998; accepted in revision 29 August 1999.*

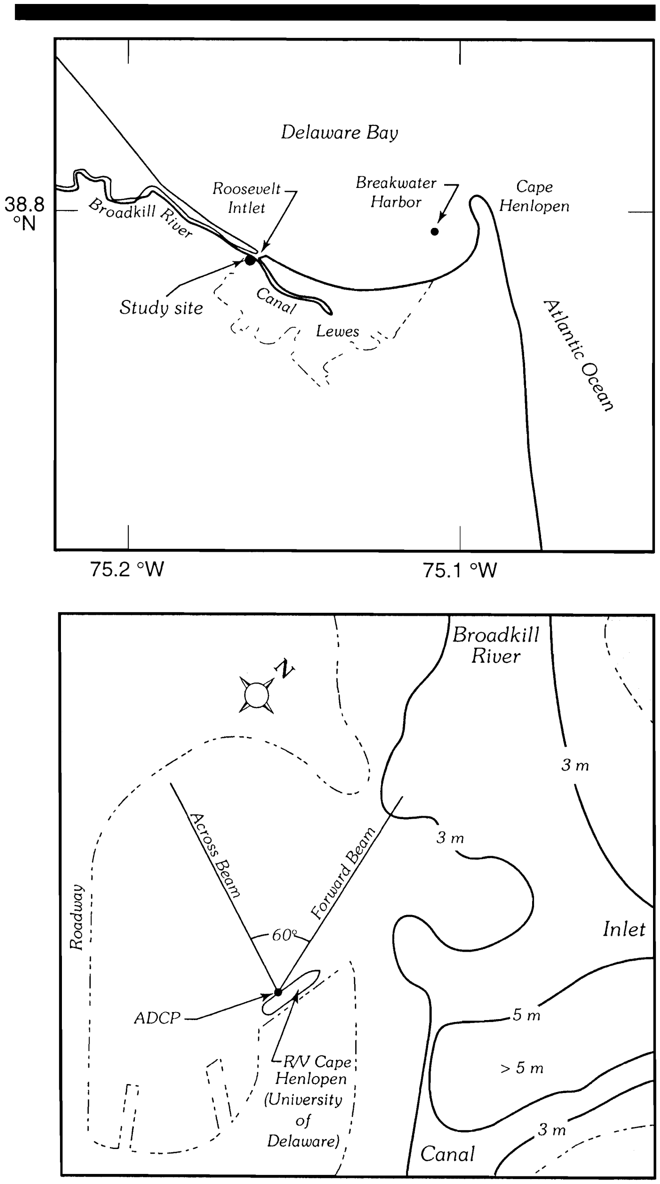


Figure 1. (Top) Study site and (bottom) sketch of ADCP deployment. Length of acoustic beams is about 120 m.

and a dry laboratory space in which to house a computer and the ADCP electronics or "deck box". However, this was not essential to the operation as battery power could have been used, the gear stored in a vehicle, and the ADCP transducer mounted on a piling or other convenient support. Such flexibility is an advantage of this approach.

The transducer was oriented so two beams were approximately horizontal. This was accomplished by first aligning the ADCP with the pole, then deploying the pole and plumbing it by using a graduated leveling device. The error in achieving a true vertical is estimated to be about 1°. To prevent interference with the horizontal beams, the remaining two ADCP transducers (lying in the vertical plane) were covered with an absorbent material. Two orthogonally positioned angle sensors were mounted above the ADCP to measure pitch and roll fluctuations. These fluctuations were less than 0.2° except during one period (1500–1700 17 May) when values of about 0.5° were recorded. These small fluctuations are ignored in the subsequent processing of the ADCP data. The azimuthal orientation transducer was adjusted by rotating the support pole so one beam (the "forward beam") pointed toward the mouth of the embayment (and towards Roosevelt Inlet), and the other (the "across") beam, being at a fixed relative azimuth angle of 60° to the forward beam, pointed approximately across the embayment (see Figure 1). The beam orientations shown in the figure are accurate to within about 10°. Also measured was the water temperature at the ADCP location but no further hydrographic data were collected. The local water level was not measured.

Each acoustic beam is shaped like a narrow cone having a spread of about 3° (0.052 rad). Thus at a range from the transducer of 23 m, the half-width of a beam is 0.6 m (equal to the transducer depth), and so the beams begin to intersect the surface. (The effect of side-lobes is ignored.) With increasing range an increasingly deeper part of the water column is insonified: to about 3-m depth at a range of 100 m. This can lead to some ambiguity about the depth of the backscattered acoustic signal and hence the depth of the measured current. Nevertheless, for all but the lightest winds, the intermittent breaking of surface gravity waves creates a layer of small air bubbles just below the surface. These microbubbles have a huge scattering cross-section and so dominate the acoustic return (*e.g.,* FARMER, 1997). The mean wind speed over the measurement period was 5.7 m/s (2.3 m/s standard deviation). Therefore, even at large ranges, we expect the data to be weighted toward the surface. An exception to this is when the beam intersects the bottom, which is clearly recognizable in the data by a large signal in the acoustic backscatter. This can occur at far range and at low water.

The Doppler velocity data were recorded from each of the two horizontal beams at a rate of 100 samples per minute using the manufacturer's data acquisition program TRANSECT. To reduce noise, the data were later averaged over 10-s, 5-min, and 30-min intervals. For a 5-min mean, the rms noise was determined to be about 1.5 cm/s. The range bin or cell size was set at 1.18 m, and 100 bins of data were collected from each beam. The first bin was centered at a range of 2.37 m from the transducer and the last bin was thus at a range of 120 m. (This is the approximate length of the beams shown in Figure 1.) However, to avoid possibly contaminated data at far range where the water is shallow and bottom scattering is more likely, attention is restricted to range of 90 m (bin 75), which is approximately three-quarters of the distance across the embayment. Also, data from the first three range bins were judged to be affected by reflection from either the ship's hull or the dock. Hence, results will be shown for only range bins 4–75 (range of about 6 to 90 m).

## Results

Figure 2 shows an overview of the measurements. These were begun at 0615 EDT on 17 May 1997 and continued through 1615 EDT on 18 May 1997, a time interval of 34.0

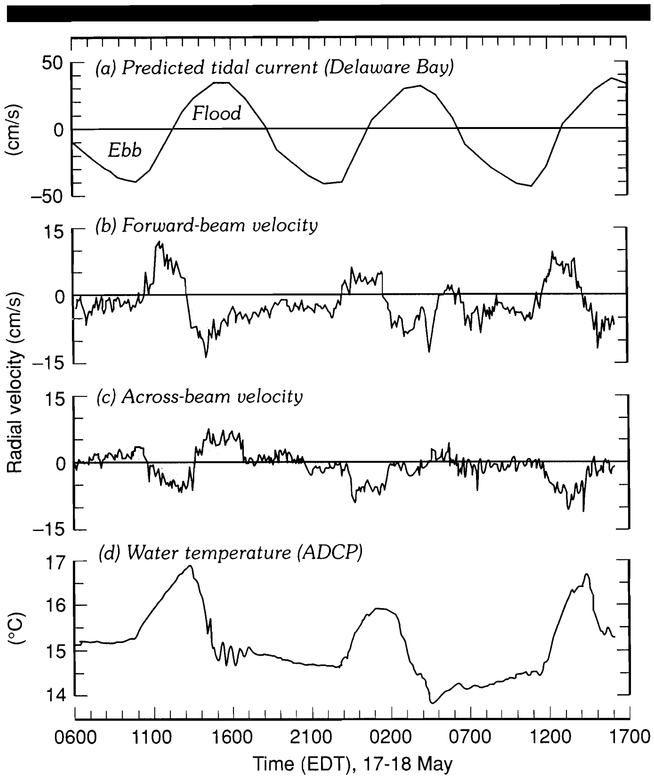


Figure 2. Time series plots of (a) predicted tidal current at Breakwater Harbor (38.793°N, 75.108°W), (b,c) radial velocity averaged over range cells 15–25, (d) water temperature measured at the ADCP transducer. Velocity vectors based on (b) and (c) are shown in a subsequent figure.

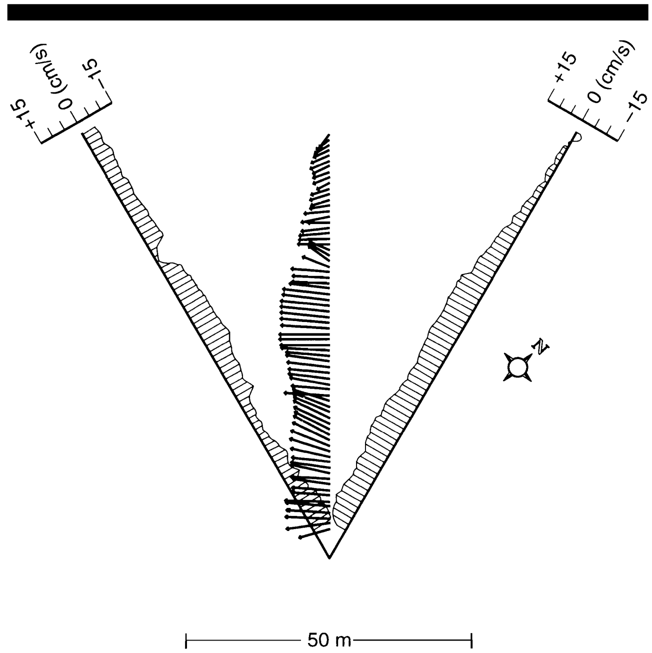


Figure 3. (Left and right) Radial velocity vs. range (6 to 90 m) for the across and forward beams averaged over 1125–1156 EDT. For the forward beam all but the last range cell show (positive) flow towards the transducer; for the across beam all the range cells show (negative) flow away from the transducer. (Middle) Mid-beam vector currents constructed by combining forward- and across-beam radial velocities for each range cell. The range-averaged current is about 15 cm/s along 235°T, *i.e.*, into the embayment.

hours or 2.74 $M_2$ tidal periods. Plotted in Figure 2a is the predicted tidal current at Breakwater Harbor, which is located just west of Cape Henlopen (Figure 1). Figure 2b and 2c show representative time series of radial velocity for the forward and across beams. In this figure the data have been averaged over range bins 15 to 25, but the full range variation of the velocity (including the velocity vector) will be shown in later figures. High-frequency fluctuations appearing in the velocity traces are uncorrelated noise and can be ignored. Figure 2d shows the near-surface water temperature as measured at the ADCP.

The measurements begin during ebb flow in the bay. At this time (prior to 1030 EDT), the radial velocity for the forward beam is slightly negative and slightly positive for the across beam. Positive (negative) radial velocity indicates a component of flow toward (away from) the ADCP. By 1130 EDT, the forward-beam radial velocity increases to about 10 cm/s while the across-beam velocity is about −5 cm/s. These signals persist for about two hours and, taken together, correspond to a surface current of about 15 cm/s flowing toward 235°T, *i.e.*, an inflow to the embayment. (Note the onset of this inflow occurs an hour before the predicted start of flood.) This is illustrated for the peak signal in the forward beam (1125 to 1156 EDT) in Figure 3, which shows the vector velocity computed by combining the radial velocity components from each beam and at each range cell and plotting it along the mid-beam centerline. This construction of a horizontal profile of vector velocity assumes that the flow streamlines have a radius of curvature that is large compared to the range from the ADCP. One can consider this as an initial working hypothesis, the validity of which can be checked later on physical grounds. Variation of signal with range (as in Figure 3) is compatible with this hypothesis; but note in Figure 3 the effect on the computed vectors of four anomalously low radial velocities in the across beam (at a range of about 65 m). This was caused by a weed bed, which appeared as a persistent band of high values of acoustic backscatter (not shown).

Further understanding of the onset of the inflow is provided by an examination of the 10-s resolution data. Figure 4 shows, for the interval 1020–1110 EDT, a grey-scale rendering of the radial velocity for each of the two beams plotted against time (x-axis) and range (y-axis). Flow in the forward beam (upper panel) is initially about −4 cm/s. This changes abruptly to a positive flow of 8 to 10 cm/s between 1032 and 1040 EDT. This change begins at far range and proceeds continuously across the plot to near range; it thus appears to represent a velocity front that translates through the beam. Values of radial velocity after 1040 EDT remain generally higher than before 1032 EDT, but the signals have a banded appearance. This range variability persists to later times (*e.g.*, to the interval 1125–1156 EDT shown in Figure 3) and

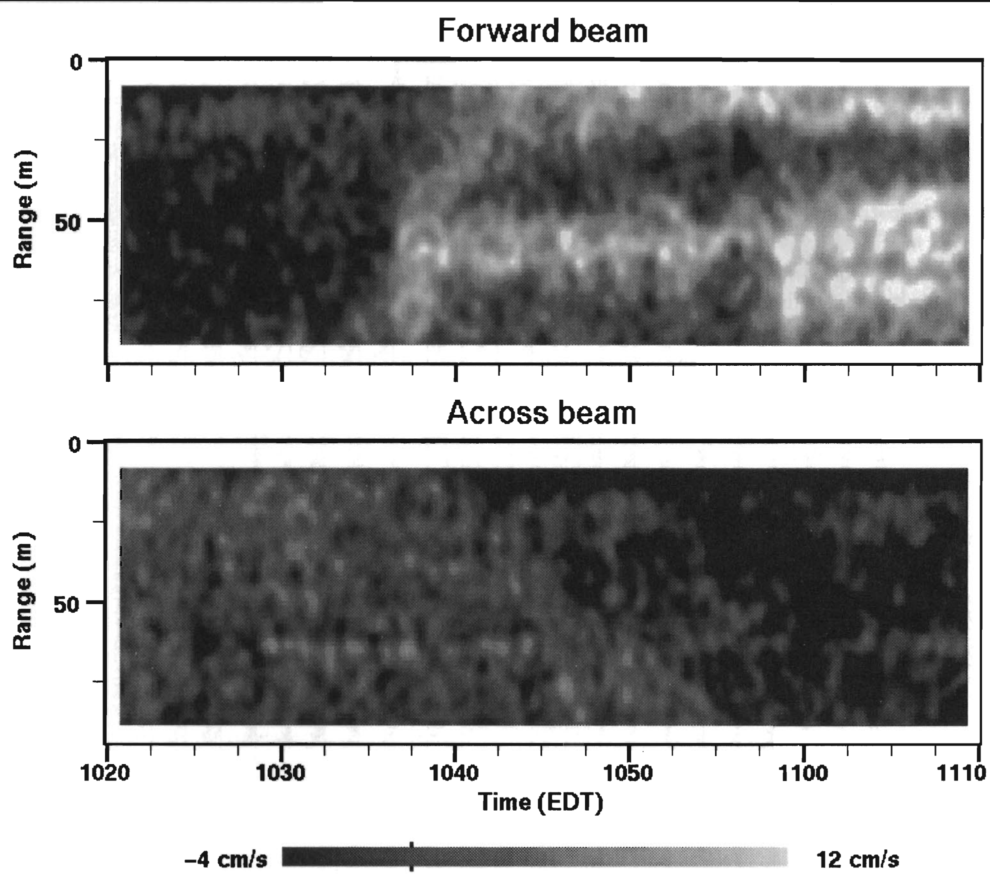


Figure 4. Time-range plots of radial velocity. The velocity range is −4 to 12 cm/s (scale shown at bottom). A positive velocity indicates flow towards the transducer. The original 10-s data have been averaged additionally with five passes of a Hanning window three time intervals wide and three range cells high. A horizontal band at about 65-m range in the lower panel shows contamination from a shallow weed bed. Sloping regions of strong velocity change indicate a velocity front that translates into the embayment about an hour before the start of flood in Delaware Bay.

implies some slowly evolving structure embedded in the flow field.

The time-range plot for the across beam (Figure 4, lower panel) shows a similar velocity frontal signal. In this case, the initial radial velocities are positive, averaging about 2 cm/s. The front now appears first at near range at about 1040 EDT (*i.e.,* continuous with its translation through the forward beam) and then extends to about 85-m range at 1055 EDT. After the front has passed, the radial velocities are about −4 cm/s. The frontal velocity jump is thus about 6 cm/s, or about half that in the forward beam. Note that the motion of the velocity front is continuous across the region of the weed bed, which appears in the plot as a horizontal band at 65-m range.

Along-beam frontal translation speeds can be calculated from the slope of the velocity jumps in the time-range plots in Figure 4. Using a straight-line fit we obtain a speed of about 23 cm/s through the forward beam and about 8 cm/s through the across beam. If we assume the frontal shape was linear and propagated in the same direction as the mean flow behind it (*i.e.,* 235°T as shown in Figure 3), then its translation speed into the embayment would be initially about 14 cm/s (through the forward beam) and then 4 cm/s (through the across beam). This spatial deceleration would be consistent with the smaller frontal velocity jump in the across beam compared to that in the forward beam. Also, a closer examination of the range-time plots in Figure 4 shows some curvature to the frontal signatures consistent with deceleration, *i.e.,* a more horizontal inclination as time progresses. At an average speed of the order of 10 cm/s, the front would cross the embayment in about 20 min. The origin of the frontal signal might be Roosevelt Inlet, from which may emanate a jet-like, radially expanding flow (*cf.* MEHTA and MONTAGUE, 1991).

After the period of strong inflow, Figure 2 shows that at about 1330 EDT the forward beam switches to negative flow while the across beam switches to positive flow. This now corresponds to essentially an oppositely pointing velocity vector. This is illustrated in Figure 5 (top panel), which shows the centerline vectors at approximately half-hour intervals throughout the first 12.4 h of the measurements. The pattern now (15th to 20th profile from the left) is one of increasing outflow at near- to mid-range. This flow pattern lasts about 3 h. Subsequently, over about 1700–2300 EDT, the radial velocities in Figure 2 weaken, the forward velocities being

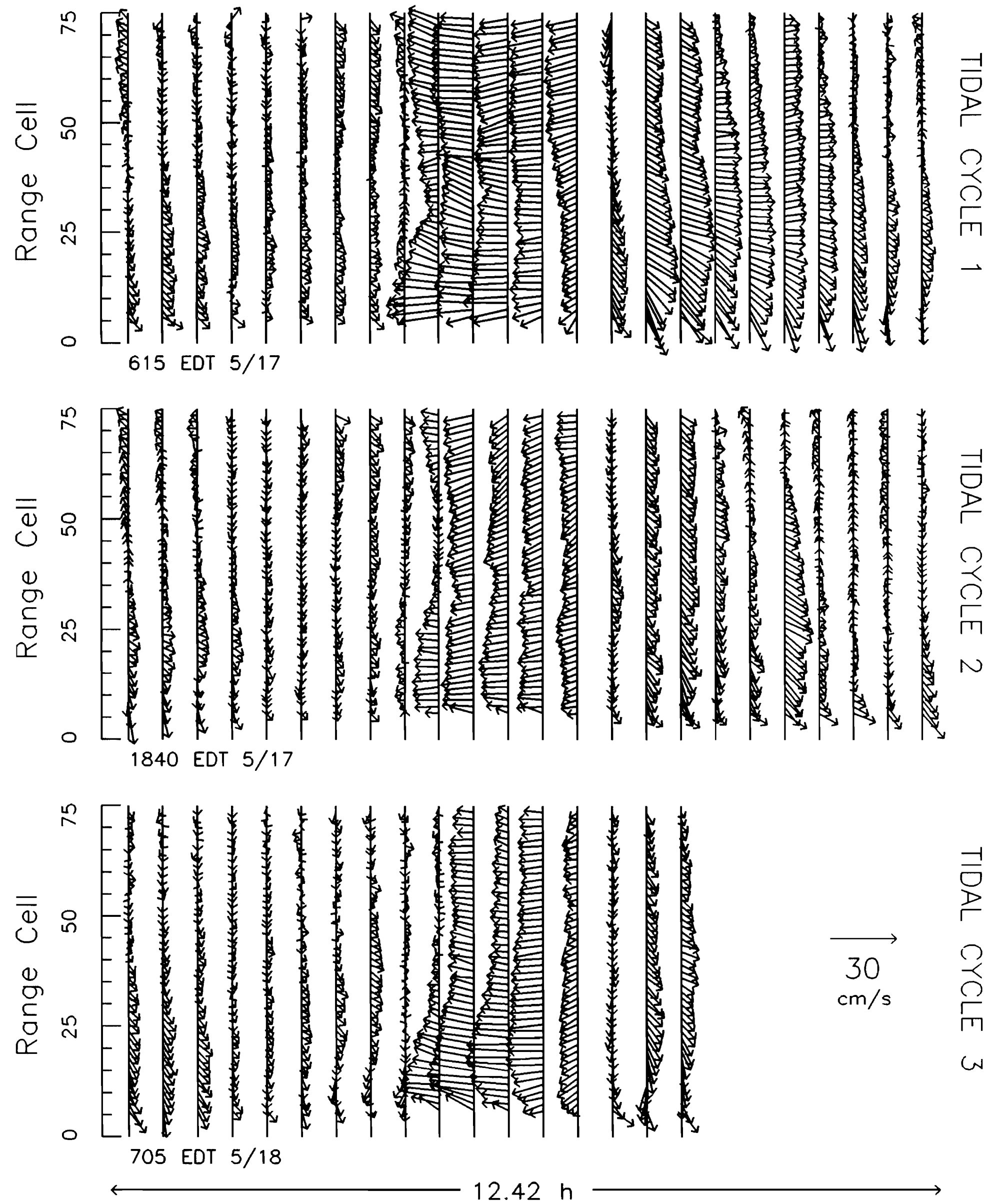


Figure 5. Time-range plots of vector currents, arranged to show the repetitive spatial patterns in the data. Each vector is an average over 31 min, and each panel is 12.42-h long. Top panel begins at 0615 EDT (May 17); middle at 1840 EDT (May 17); bottom at 0705 EDT (May 18). Range cells 4–75 are shown. The 11th profile in the top panel corresponds that shown in Figure 3. Anomalous vectors are due to shoal regions.

slightly negative and the across velocities near zero, similar to the initial few hours of the measurements. The velocity vectors in Figure 5 (beginning and end of the top panel) show reverse-directed flows at near and far range, indicating a possible recirculating or eddy-like flow pattern in the embayment (see below).

Basically the same sequence of events as above is repeated over the subsequent two tidal cycles. Periods of positive flow in the forward beam and negative in the across beam (Figure 2, centered at 0045 EDT and 1315 EDT) commence roughly one hour before the predicted start of flood in the bay. Each of these periods is followed by a period of negative flow in the near range of the forward beam and positive flow in the across beam. The spatial flow patterns are compared in Figure 5 for each successive tidal cycle as measured from the start of the measurements. A repetitive signal is seen as well in the trace of water temperature (Figure 2).

Such repetitive patterns provide a measure of confidence that the signals are real ones related in some way to local tidal forcing. Also, the period of relatively strong inflow is approximately in balance with the time-integrated outflow over each tidal cycle. However, a more interesting aspect of the measurements is revealed when one tries to balance either inflow or outflow of mass (based on Figure 5) with the expected tidal range of water level of about 1 m. For example, assume inflow lasts for $\Delta t \approx 2.5$ h and that the depth-averaged flow through the mouth $\langle u \rangle \approx 7$ cm/s, *i.e.,* half the average surface velocity shown in Figure 5. The integrated rise in water level can then be estimated as $\Delta\eta \approx \langle u \rangle\ \Delta t$ times the ratio of the mouth cross-sectional area (175 $m^2$) and embayment surface area ($2 \times 10^4$ $m^2$). This gives $\Delta\eta = 5.5$ m, or nearly a factor-of-six too large!

The anomalously high range calculated above can be reconciled by assuming the existence of either a lower-layer compensatory flow or a particular pattern of recirculatory surface current. One possibility is the existence of two counter-rotating eddies inside the embayment as follows. During late ebb and early flood, a clockwise (outer) eddy is driven (perhaps through entrainment) by down-river flow outside the mouth, thus accounting for the positive radial velocities measured in the forward beam, while a counter-clockwise (inner) eddy lies farther in the embayment guided by the strongly curving southern coastline, thus accounting for the negative radial velocities measured in the across beam. During this period the temperature measured at the ADCP position gradually increases (Figure 2d). Approximately 1 h into flood, we speculate there is a reversal of the rotation of these eddies such that the outer eddy is now driven by upriver flow; the reversal coincides with an abrupt decrease in the measured temperature. Note that the existence of such eddies would violate the earlier working hypothesis; thus in this case combining the two beams into a single horizontal profile would be unwarranted.

## Summary and Discussion

A preliminary study has been made of the horizontal structure of near-surface currents in a small embayment using a standard ADCP deployed at a single shore location. The measurements suggest that inflow to the embayment begins abruptly (as a velocity front) about 1 h before predicted flood and that, over much of the tidal cycle, an eddy-like circulation pattern is present that may be driven by a riverine flow at the embayment's mouth that is itself tidally modulated. As a result, the flow shows a complex behavior in both space and time. The approach has the advantages that the instrument is generally out of harm's way and accessible to the investigator should it need to be adjusted, and that, because the data are recorded ashore, monitoring of the currents in near real-time is possible. Also, in addition to the velocity measurements emphasized in this report, acoustic backscatter data recorded by the ADCP may also be useful in some applications, for example, as an indicator of sediment transport.

A shortcoming is the use of spatially disparate radial velocity measurements to synthesize a velocity vector. We have used a very simple approach, *i.e.,* combining the beam-pair radial velocities, but this will generally be inadequate for flows having significant curvature; therefore, an alternative sampling or analysis approach may be needed for some investigations. An improvement might be to use an ADCP having a smaller beam separation angle. (In our measurements it was 60°, making the intra-beam separation equal to range from the ADCP.) Also, in cases where radial velocities can be measured along more than two horizontal beams, an alternative analysis scheme such as that of FORRISTALL (1996) might be employed.

Despite the potential drawbacks, we believe horizontal ADCP velocity measurements can still serve as a useful exploratory probe of the circulation. This has been illustrated by the present study, which showed several interesting and unanticipated results.

## ACKNOWLEDGMENTS

The measurements were made over a weekend layover during the Chesapeake Bay Outflow Plume Experiment (COPE-2), which was part of the Physics of Coastal Remote Sensing Accelerated Research Initiative, funded by the Office of Naval Research and managed at NRL by Dr. Richard Mied. Tim Pfeiffer, Director of Marine Operations, University of Delaware, and Matt Hawkins, Master of the R/V Cape Henlopen, provided technical assistance and information about the local water circulation.

## LITERATURE CITED

FARMER, D.M., 1997. Observing the ocean side of the air-sea interface. *Oceanography,* 10(3), 106–110.

FORRISTALL, G.Z., 1996. Measurements of current blockage by the Bullwinkle Platform. *Journal of Atmospheric and Oceanic Technology,* 13(6), 1247–1266.

MEHTA, A.J. and MONTAGUE, C.L., 1991. A brief review of flow circulation in the vicinity of natural and jettied inlets: Tentative observations on implications for larval transport at Oregon Inlet, NC *Report UFLICOELIMP91/03.* Coastal and Oceanographic Engineering Department, University of Florida, Gainesville, Florida, 74p.

MORANG, A., LARSON, R., and GORMAN, L., 1997. Monitoring the coastal environment; Part I: Waves and currents. *Journal of Coastal Research,* 13(1), 111–133.

PADUAN, J.D. and COOK, M.S., 1997. Mapping surface currents in Monterrey Bay with CODAR-type HF radar. *Oceanography,* 10(2), 49–52.

PRANDLE, D., 1997. Tidal and wind-driven currents from OSCR. *Oceanography,* 10(2), 57–59.